Shaoyong Yu[1]
Ping Yao[1]
Ming Jiang[1]
Guangzhao Zhang[2]
[1] *The Key Laboratory of Molecular Engineering of Polymers and Department of Macromolecular Science, Fudan University, Shanghai 200433, China*

[2] *The Open Laboratory of Bond Selective Chemistry, Department of Chemical Physics, University of Science and Technology of China, Hefei, Anhui 230026, China*

Nanogels Prepared by Self-Assembly of Oppositely Charged Globular Proteins

Received 28 December 2005; revised 4 April 2006; accepted 7 May 2006
Published online 22 May 2006 in Wiley InterScience (www.interscience.wiley.com). DOI 10.1002/bip.20539

Abstract: *Ovalbumin and lysozyme are two main proteins in hen egg white with the isoelectric points of 4.8 and 11, respectively. Herein we report the manufacture of stable, narrowly distributed nanogels (hydrodynamic radius about 100 nm) using a novel and convenient method: ovalbumin and lysozyme solutions were mixed at pH 5.3, the mixture solution was adjusted to pH 10.3, then subsequently stirred and heated. The nanogels were characterized using a combination of techniques. The nanogels have spherical shape and core-shell structure. The core is mainly composed of lysozyme and the shell is mainly composed of ovalbumin. The proteins in the nanogels are in denatured states and they are bound by intermolecular hydrophobic interactions, hydrogen bonds, and disulfide bonds. The charges of the nanogels can be modulated by the pH of the medium. The electrostatic repulsion of ovalbumin molecules on the nanogel surface stabilizes the nanogels in aqueous solution. The formation mechanism of the nanogels is discussed.* © 2006 Wiley Periodicals, Inc. Biopolymers 83: 148–158, 2006

This article was originally published online as an accepted preprint. The "Published Online" date corresponds to the preprint version. You can request a copy of the preprint by emailing the Biopolymers editorial office at biopolymers@wiley.com

Keywords: *lysozyme; ovalbumin; nanogel; self-assembly*

INTRODUCTION

Biological self-assembly provides illustrations of thermodynamically stable supramolecular arrays that not only have regular architectures but also have intelligent functions.[1] Inspired by the convenience of organizing molecules via noncovalent associations, self-assembly has undoubtedly been an active field of

Correspondence to: Ping Yao; e-mail: yaoping@fudan.edu.cn
This article includes supplementary material available at http://www.interscience.wiley/com/jpages/0006-3525/suppmat

current chemistry and has found wide application.[2–6] Among all of the building blocks suitable for self-assembly, many researchers concentrate on the synthetic molecules and have obtained many results[7–9]; on the other hand, many researchers use DNA, proteins, lipids, and even viruses to fabricate potential biological materials.[6,10–12] For example, Cao and Armitage et al. synthesized and characterized thermoreversible biopolymer microgels based on hydrogen bonding of DNA and recoverable enzymatic microgel based on biomolecular recognition.[13,14] Clark et al.[11] recently reviewed nanoscale self-bioassemblies using the linkers of nucleic acid complementarity and protein specific interactions, such as antigen and antibody, streptavidin and biotin. However, there are few researchers studying the self-assembly of the proteins without the linkers of specific interactions in aqueous solution. The reasons are as follows: when two oppositely charged proteins are mixed, structureless aggregates or precipitates form; when two proteins with the same charges are mixed, electrostatic repulsion results in no complex forming; when the proteins are in a denatured condition, only fibril,[15–17] gel, and coagulation[18] form.

Food proteins have many functions, such as lipid and flavor binding and retention, gelation, and emulsification.[19] Therefore, food proteins are ideal materials to fabricate nanoparticles for drug delivery. Gelation of food proteins is an important property and has been discussed in many articles.[20] The gelation process follows three steps after the initial heat-denaturation of the food protein[18]: the formation of aggregates via hydrophobic interaction, the stiffening of the aggregates through sulphydryl–disulfide reaction, and a large increase in elasticity resulting from the formation of multiple hydrogen bonds upon cooling. Proteins are polyampholytes and their charges and hydrophobicity/hydrophilicity are pH dependent. Protein hydrogel is a network cross-linked by hydrophobic interaction and disulfide bonds and hydrogen bonds.[21] It is reasonable to think that food protein hydrogels with nanoscale dimensions are ideal candidates for loading and releasing drugs as synthetic polymer microgels and micelles have demonstrated, because the pH response property of the gel offers reversible sites to bind and release drugs, the low density and network property offer more space and binding sites to load drugs, the cross-linking property can suppress dissociation upon dilution, and the nano- or microsize can respond to the environmental stimulation immediately.[2,22,23] However, as far as we know, there is no report on nanogels produced with proteins solely.

Ovalbumin and lysozyme are two main proteins in hen egg white. In detail, ovalbumin is a monomeric phosphoglycoprotein, it consists of 385 amino acid residues, the molecular weight is 47,000 Da, and the isoelectric point (pI) is 4.8.[21] The ovalbumin molecule has one internal disulfide bond and four free sulphydryl groups. It has an ellipsoidal shape with dimensions of $7 \times 4.5 \times 5$ nm (PDB: 1OVA).[18] Lysozyme is a well-known enzyme that has the ability to cause lysis of bacterial cells.[24] The lysozyme molecule has 129 amino acid residues, molecular weight of 14351 Da, pI of 11,[21] four internal disulfide bonds, and an ellipsoidal shape with dimensions of $3.8 \times 2.4 \times 2.2$ nm (PDB: 2LYZ). Matsudomi et al.[25] have reported heat-induced aggregation between ovalbumin and lysozyme at neutral pH, which was caused by electrostatic attraction, and sulphydryl–disulfide interchange between the heat-denatured protein molecules. Heating ovalbumin or lysozyme solution individually, transparent solution, turbid suspension, transparent gel, translucent gel, or opaque gel was obtained depending on the concentration of the protein, pH and ionic strength of the solution.[26,27] In this article, we use a convenient method to assemble ovalbumin and lysozyme, two oppositely charged globular proteins, to narrowly dispersed nanogels. The nanogels are characterized using a combination of techniques. The formation mechanism of the nanogels is discussed.

MATERIALS AND METHODS

Materials

Egg white ovalbumin from Sigma Chemical Co. (St. Louis, MO; grade IV) and egg white lysozyme from Sino-American Biotechnology Co. (Shanghai, China) were used without further purification. All other reagents with analytical grade were purchased commercially and used as received. All samples were prepared with deionized water purified to a resistance of 17–18 MΩ.

Nanogel Preparation

Ovalbumin aqueous solution (43 μM) was added dropwise into lysozyme aqueous solution (43 μM) with gently stirring until final molar ratio (MR) of ovalbumin to lysozyme 0.4 was obtained. After the two proteins were mixed, the pH of the mixture reached 5.3. Then the pH of the mixture was adjusted to 10.3 with 1M NaOH. After gentle stirring for 1 h and then heating at 80°C for 90 min, a homogeneously dispersed nanogel solution was obtained. The procedure shown here is a standard one; the other conditions used in this report will be specially indicated.

Quartz Crystal Microbalance-Dissipation (QCM-D) Measurement

Individual ovalbumin or lysozyme was dissolved in phosphate buffered saline (PBS) solution (10 mM phosphate

buffer with 0.10*M* ionic strength, pH 7.2 or 10.3) to obtain ovalbumin- or lysozyme-buffered solution with a concentration of 71.4 μM. QCM-D measurements were performed on a commercial multifrequency quartz crystal microbalance Q-Sense D300 (Q-Sense AB, Gothenburg, Sweden). Gold-coated electrode was cleaned in a 1:3 mixture of H_2O_2 and H_2SO_4 at 80°C for 30 min and rinsed with deionized water, acetone, and ethanol in sequence, then immersed into freshly prepared $1 \times 10^{-4} M$ 1-dodecanethiol [$HS(CH_2)_{11}CH_3$] absolute ethanol solution for 18 h under gentle stirring. The modified electrode was washed with ethanol and deionized water, and subsequently exposed to moderate nitrogen gas flow to dry. After mounting the dodecanethiol-modified electrode, the initial resonant frequency f and dissipation factor D were recorded as the baseline, then lysozyme PBS solution flowed through the modified electrode surface. After a period of deposition of lysozyme, the electrode was flushed with PBS solution, and then the ovalbumin PBS solution flowed through the lysozyme-absorbed electrode surface followed by a washing step.

Dynamic Light Scattering (DLS) Measurement

Malvern Autosizer 4700 (Malvern Instrument, Worcs, UK) equipped with a multi-τ digital time correlator (Malvern PCS7132) and Compass 315M-100 Diode-Pumped Laser (Coherent, Inc., Santa Clara, CA; output power >100 mW, $\lambda_0 = 532$ nm) as light source was used to perform the DLS measurement. The linewidth distribution $G(\Gamma)$ was calculated from the Laplace inversion of the measured intensity–intensity time correlation function by a CONTIN program. The polydispersity index (PDI, $\langle \mu_2/\Gamma^2 \rangle$) was also obtained by the CONTIN program. $G(\Gamma)$ can be converted into the translational diffusion coefficient distribution $G(D)$ or a hydrodynamic radius distribution $f(R_h)$. All the measurements were performed at 25°C and at a scattering angle 90° for the purpose of comparing relative changes of the particle size conveniently; thus the hydrodynamic radius obtained was an apparent z-averaged hydrodynamic radius $\langle R_h \rangle$, simply written as R_h. Real hydrodynamic radius $\langle R_h \rangle_{real}$ was obtained via extrapolating the scattering vector to zero degree scattering angle after a measurement at an angle range from 90° to 15°.

Static Light Scattering (SLS) Measurement

A modified commercial laser light scattering spectrometer (ALV/SP-125, Laservertriebsgesellschaft, Langen, Germany) equipped with a multi-τ digital correlator (ALV-5000) and a solid-state laser (DPY425II, ADLAS, Lübeck, Germany; output power ~400 mW at $\lambda_0 = 532$ nm) was used to perform static light scattering measurement. The z-averaged root mean square radius of gyration ($\langle R^2_g \rangle^{1/2}$ or simply written as $\langle R_g \rangle$) can be determined from the angular dependence of the Rayleigh ratio.[28] The solutions with the concentration of 9.47×10^{-5} g/mL were cleaned using 0.8 μm Millipore Millex-LCR filter to remove dust. The measurement was performed at 25°C with the angles from 15° to 60° at an interval of 1°. The dn/dC value of 0.167 was determined using an Optilab DSP differential refractometer (Wyatt Technology Corporation, Santa Barbara, CA).

Transmission Electron Microscopy (TEM) Measurement

TEM imaging was performed on a Philips CM 120 electron microscope (FEI Company, Hillsboro, OR) at an accelerating voltage of 80 kV. The specimens were prepared by dropping solution onto copper grids coated with carbon film and followed by natural drying or lyophilization.

ζ-Potential Measurement

ζ-Potential measurement was carried out at 25°C with Zeta-Sizer Nano ZS90 (Malvern Instrument, Worcs, UK) equipped with MPT-2 Autotitrator and 4 mW He-Ne Laser ($\lambda_0 = 633$ nm) based on the technique of Laser Doppler Electrophoresis. The electrophoresis mobility U_E was measured and the zeta potential ζ was calculated by the Henry equation,[29] $U_E = (2\varepsilon\zeta/3\eta)f(ka)$, where ε, η, $f(ka)$ were the dielectric permittivity of the solvent, viscosity of the solution, and Henry's function. The value of $f(ka)$ here was determined to be 1.5, according to Smoluchowski approximation.[30,31]

Isolating Nanogels from Solution Using a High Flow Ultrafiltration Membrane

Samples filled in Microcon YM-100 [molecular weight cut-off: 1×10^5; Millipore (Shanghai) Trading Co., Ltd., Shanghai, China] vessels were centrifugated at 3000× g for 15 min to isolate nanogels from solution. The individual protein molecules ($M_w < 1 \times 10^5$), which did not take part in the nanogel assembly, flowed through the membrane and were collected as filtrate; the nanogels remained in vessels.

Gel Electrophoresis

Sodium dodecyl sulfate–polyacrylamide gel electrophoresis (SDS-PAGE) was carried out on a gel electrophoresis apparatus (JM250, JM-X Scientific Company, Dalian, China). The gel was stained with Coomassie Brilliant Blue and the protein content in each track was analyzed using the standard gray scale analysis method provided by Origin software (OriginLab Corp., Northampton, MA).

RESULTS

Nanoparticle Preparation

As mentioned above, the pI is 4.8 for ovalbumin and 11 for lysozyme. The electrostatic attraction between

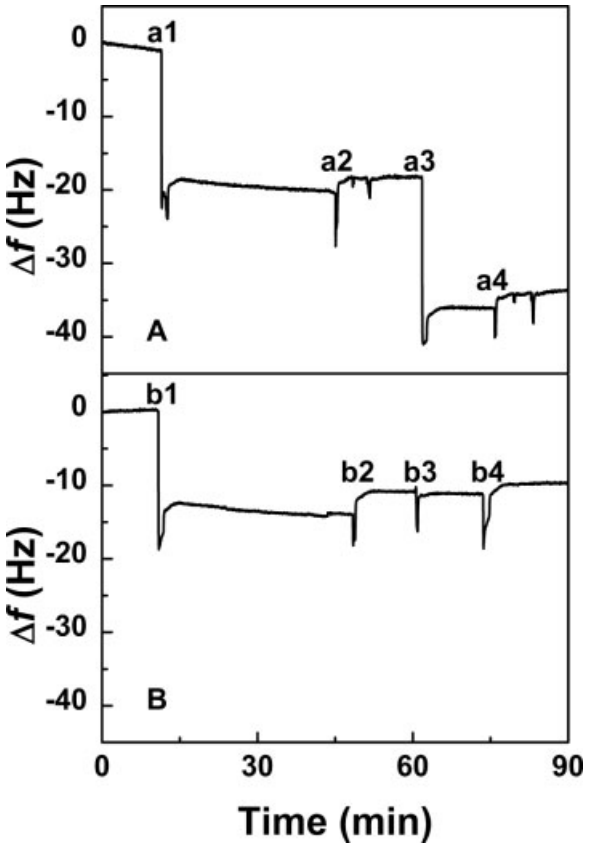

FIGURE 1 QCM response for the sequential adsorption of lysozyme and ovalbumin onto 1-dodecanethiol modified gold electrode surface at pH 7.2 (A) and pH 10.3 (B). The markers denote the protein or buffer added: a1, lysozyme (pH 7.2); a2, PBS (pH 7.2); a3, ovalbumin (pH 7.2); a4, PBS (pH 7.2); b1, lysozyme (pH 10.3); b2, PBS (pH 10.3); b3, ovalbumin (pH 10.3); b4, PBS (pH 10.3).

these two proteins may occur in the pH range of 4.8–11, where they carry opposite charges; when solution pH is close to the pI value of lysozyme, the electrostatic attraction or electrostatic repulsion between these two proteins may be weak because the net charges of lysozyme is about zero. This speculation is proved by QCM-D study in which the response signal changes of resonant frequency f and dissipation factor D are generally assumed to be proportional to the mass of substance bound to the electrode surface.[32] Figure 1 shows resonant frequency f response for the sequential adsorption of lysozyme and ovalbumin onto the 1-dodecanethiol modified gold electrode surface at pH 7.2 (A) and pH 10.3 (B). The adsorption of ovalbumin on the lysozyme adsorbed surface at pH 7.2 is totally different from that at pH 10.3: ovalbumin strongly interacts with the adsorbed lysozyme at pH 7.2 but does not so at pH 10.3. This result means that there is strong electrostatic attraction between ovalbumin and lysozyme at pH 7.2, but the attraction does not exhibit at pH 10.3. In theory, the electrostatic attraction exists because the pI is 4.8 for ovalbumin and 11 for lysozyme; possibly, the attractive interaction is too weak to overcome translational entropy loss to immobilize ovalbumin at pH 10.3. Besides, Figure 1 shows that the lysozyme adsorbed on electrode surface is smaller at pH 10.3 than that at pH 7.2. This is because the gold electrode surface carries negative charges, although it is modified with 1-dodecanethiol [$HS(CH_2)_{11}CH_3$] and the net positive charges of lysozyme decrease to near zero when the pH varies from 7.2 to 10.3. So, the decrease of electrostatic attraction between the electrode and lysozyme causes the decrease of the adsorption of lysozyme at pH 10.3.

However, we found that it was impossible to produce homogeneously dispersed particles composed of ovalbumin and lysozyme by simply mixing their solutions at any pH and any ratio directly. For example, when the two proteins were mixed at acidic pH, which is close to the pI of ovalbumin, or mixed at alkaline pH, which is close to the pI of lysozyme, the resultant mixture was transparent, suggesting that soluble complexes formed or there was no complexes formed because of the electrostatic repulsion between ovalbumin and lysozyme; when the two proteins were mixed at neutral pH, the precipitation occurred because of strong electrostatic attraction.

After heat treatment, the interactions between the two proteins are more complicated. Generally, heat-induced protein denaturation causes proteins to lose their compact structure, to expose their hydrophobic residues to the surface, and to exchange their disulfide bonds,[26] resulting in intermolecular hydrophobic interactions and disulfide bonds. These usually produce permanent or irreversible combination between protein molecules. Our experiment has proven that ovalbumin or lysozyme alone cannot form homogeneous nanoparticles by heat treatment at any condition. We found that heating at acidic pH, coagulation and transparent solution occurred for ovalbumin and lysozyme, respectively, while transparent solution and coagulation occurred for ovalbumin and lysozyme respectively after the heat treatment at alkaline pH. These results are the same as reported in the literature[26,27] indicating that when protein is heated at the pH away from its pI, electrostatic repulsion makes protein molecules move away from each other; when protein is heated at the pH close to its pI, the protein molecules tend to aggregate.

Furthermore, we could not obtain homogeneous particle dispersion by mixing ovalbumin and lysozyme at any pH directly and then heating the mixture.

For example, when the proteins were mixed at pH 10.3 and then heated, ovalbumin could not prevent lysozyme from coagulation because there was no significant electrostatic attraction between them as proven by QCM study (Figure 1). Similarly, coagulation happened when mixing the solutions at pH 5.3 and then heating the mixture. In addition, our and other groups' studies have found that lysozyme made insoluble aggregates with ovalbumin after heat treatment at neutral pH.[25,33]

During the experiments, we found that when the pH of the mixture was adjusted from acidic to neutral pH, the aggregates occurred; if the mixture were left at neutral pH for an hour or so, precipitation happened; when the pH of the mixture was further adjusted to the alkaline range and then the mixture stirred, the precipitates gradually dissociated. To obtain a homogeneous complex particle solution, we developed a three-step procedure: ovalbumin and lysozyme solutions were mixed at acidic pH, the mixture pH was adjusted to alkaline, and then subsequently stirred and heated for 90 min at 80°C, which is above the denaturation temperature of the proteins. Scheme 1 illustrates the summary results of heating individual ovalbumin, lysozyme, and their mixture at different pHs. The following study is to explore the suitable conditions for the particle preparation, which are pH, molar ratio of the two proteins, and stirring time.

After the two proteins were mixed with the molar ratio of ovalbumin to lysozyme (MR) 0.4, the mixture pH was 5.3 naturally. Then the mixture pH was adjusted to different alkaline values. Afterwards, the mixture at a given pH was stirred for 60 min and heated at 80°C for 90 min. Table I shows the result of DLS measurement for the final particle solutions. The data show that the size of the resultant particles is strongly dependent on the medium pH. At pH 10.3, the scattering light intensity goes up to its maximum, the hydrodynamic radius (R_h) is about 77 nm, which is close to its minimum, and the polydispersity index (PDI) is minimum, suggesting that the particle number is the largest and the particle solution is homogeneous. When the pH is lower than 9.5 and higher than 10.5, the particle solutions exhibit much lower scattering light intensity and larger PDI (multiple particle peaks). These results demonstrate that the pH of 9.5–10.5 is suitable and pH 10.3 is optimal for the particle preparation.

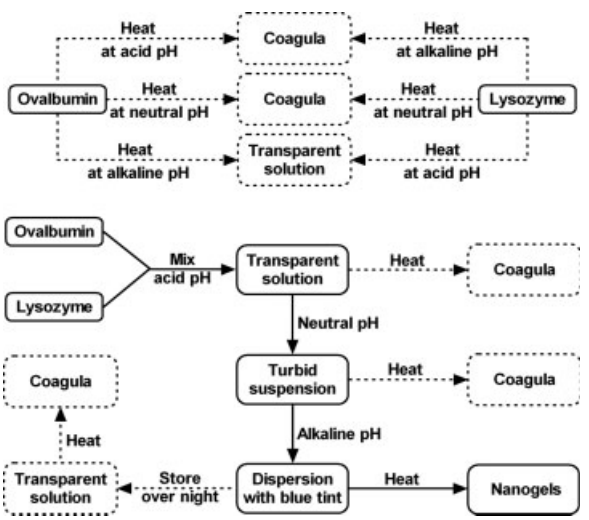

SCHEME 1 Summary results of heating individual ovalbumin, lysozyme, and their mixtures at different pHs. The protein concentration is 43 μM for each sample.

Table I DLS Result of the Particle Solutions Prepared at Different pHs[a]

pH	Intensity (Kcps)	R_h (nm)	PDI
8.0	126	1146	1.00
8.6	145	573	0.77
9.0	119	479	1.00
9.5	162	302	0.37
10.0	279	128	0.14
10.3	378	77	0.14
10.5	153	70	0.26

[a] The particle samples were produced by mixing ovalbumin and lysozyme solutions at pH 5.3 with MR 0.4, stirring at indicated pH for 60 min, and heating at 80°C for 90 min.

The interaction of ovalbumin with lysozyme depends on not only pH but also MR. Table II shows the influence of MR in the particle preparation on the

Table II DLS Result of the Particle Solutions Prepared with Different MR of Ovalbumin to Lysozyme[a]

MR	Intensity (Kcps)	R_h (nm)	PDI
0.1	98	315	0.36
0.2	150	175	0.16
0.3	212	145	0.15
0.4	321	77	0.14
0.5	302	81	0.15
0.6	287	78	0.16
0.7	215	65	0.15
0.8	92	61	0.37
0.9	68	65	0.51
1	67	60	0.39

[a] The particle samples were produced by mixing the protein solutions at pH 5.3, adjusting the pH to 10.3, stirring for 60 min, and heating at 80°C for 90 min.

scattering light intensity, R_h, and PDI of the particles. All the samples have the same concentration, 43 μM. The data in Table II show that as MR increases, the intensity increases initially and reaches the maximum at MR 0.4, then decreases sharply. Table II also shows that when MR increases the particle size decreases rapidly at first then changes insignificantly when MR exceeds 0.4. As we know, the scattering light intensity is related to particle number, particle size, and refractive index difference between solution and particle. We notice that at MR 0.4, the particle size is close to the minimum while the intensity reaches its maximum, which means that the self-assembly of these two proteins at MR 0.4, i.e., the weight ratio of ovalbumin to lysozyme 1.3, is most effective. In fact, in a broad MR range of 0.2–0.7, we can obtain stable particle solution with a narrow size distribution.

In order to understand the influence of the stirring time at pH 10.3 before the heat treatment on the final particle dispersion, the dependence of the particle size distribution and scattering light intensity on the stirring time were investigated (Figure 2). The DLS results show that the R_h value of about 77 nm does not change significantly from 0 to 330 min stirring, but the intensity decreases sharply, aggregation peak begins to appear after 120 min stirring, and more and larger aggregates appear when further increasing the stirring time, suggesting a decrease of the particle number. The stirring speed does not have definitive influence on the particle size. The reason is that similar results can be obtained whether the samples undergo standing or stirring at pH 10.3. Therefore, we choose gentle stirring at pH 10.3 for 60 min as a standard stirring condition.

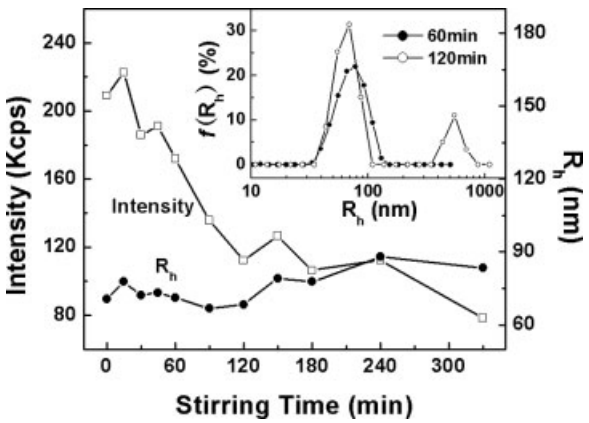

FIGURE 2 The influence of stirring time at pH 10.3 before heating on the particle size and scattering light intensity. The samples were prepared according to the standard procedure but with different stirring time before heating at pH 10.3. Inset is the size distributions of the particles prepared with 60 and 120 min stirring.

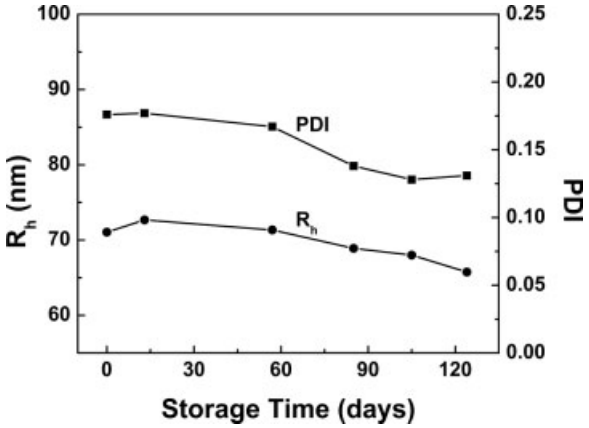

FIGURE 3 Time course of the hydrodynamic radius and polydispersity index of the particles. The sample was produced using the standard method.

The observation above reveals a suitable condition for the preparation of homogeneous ovalbumin–lysozyme nanoparticle dispersion. The particles studied below were produced using this standard process: the two protein solutions were mixed at pH 5.3 with MR 0.4; the mixture solution was adjusted to pH 10.3 and then subsequently stirred for 60 min and heated at 80°C for 90 min. The particles produced using this standard process are very stable and reproducible: the R_h is 77 ± 10 nm; PDI is 0.14 ± 0.04; the error bar of the scattering light intensity is about 5%. Figure 3 displays the changes of R_h and PDI of the particles with storage time. It is interesting to find that a reproducible $f(R_h)$ of the particles was obtained when it was monitored over a period as long as 120 days. This is no doubt a valuable character of the nanoparticles and provides a possibility for practical applications. Another advantage is that the particles can be stored as lyophilized powder and the sample does not change its size distribution very much after lyophilization and rehydration. Figure 4 shows that the intensities of the lyophilized and original particle solutions are somewhat different; perhaps, a limited aggregation exists after the lyophilized particle powder was directly dispersed in water.

Morphology and Hydrogel Structure of the Nanoparticles

The apparent hydrodynamic radii shown above were all measured at a scattering angle 90° because it is very convenient to compare the relative changes of the size in the exploring process of the particle preparation. Considering the relative large particle size, the

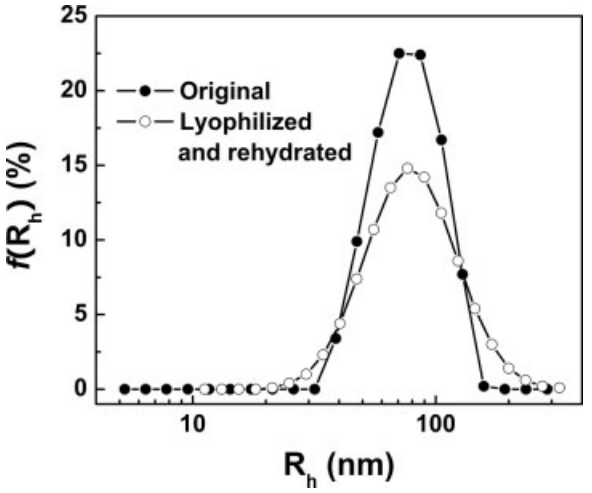

FIGURE 4 Size distributions of the particles before and after lyophilization. The sample was produced using the standard method.

angular dependence of diffusion coefficient was investigated and the *z*-averaged real hydrodynamic radius $\langle R_h \rangle_{real}$, 112 nm, was obtained for the particles prepared using the standard method.

The particle size and morphology can be verified by TEM imaging. Figure 5 shows that the particles are spherical and some particle aggregates exist. The aggregates might occur during the drying process because DLS measurements showed a narrow particle size distribution (PDI 0.14) in solution. A statistics on the particle size gives an average diameter of 80 nm, which is much smaller than that measured by the DLS (real hydrodynamic diameter 224 nm). This can be attributed to the shrinkage of the particles after water evaporation because DLS provides the data for the particles swollen in solution, while TEM shows the image of dried particles. The volume of the particles shrinks about 22 times, that is, the swelling ratio of the particles is 22. The high shrinkage indicates that the particles have a low-density structure and can contain a large amount of water in it.

A combination of dynamic and static light scattering can provide information on the particle structure. The ratio $\langle R_g \rangle / \langle R_h \rangle_{real}$ is a sensitive structure parameter: 0.774 for a uniform hard sphere; 1.5 for a random coil; 1.1 for a hyberbranched cluster, a hollow sphere or a micelle with low density structure.[28,34,35] From the angular dependence of diffusion coefficient, $\langle R_h \rangle_{real}$ 112 nm was obtained via DLS measurement as mentioned above; from the angular dependence of Rayleigh ratio, $\langle R_g \rangle$ 124 nm was calculated through static light scattering measurement. Therefore, the ratio of $\langle R_g \rangle / \langle R_h \rangle_{real}$ 1.1 was obtained for the particles. As atomic force microscopy (data not shown) and TEM (Figure 5) results exclude hollow structure, we are inclined to think that the particles have a low-density structure. Considering that the particles contain a large amount of water and both ovalbumin and lysozyme can form hydrogel on heat treatment, we tend to think that the particles have a nanogel structure, i.e., the hydrogel structure with nanoscale.

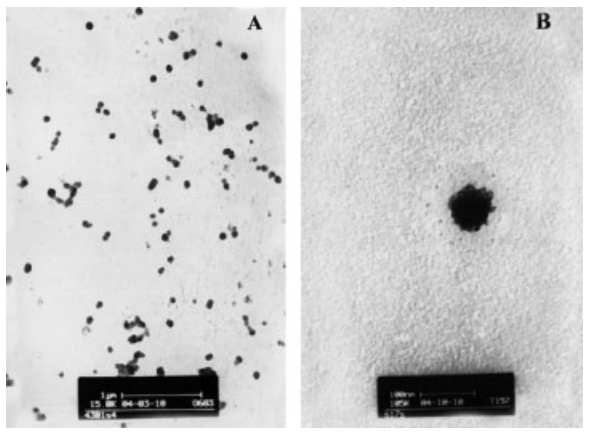

FIGURE 5 TEM images of the particles obtained using the standard method. The scale bar is (A) 1 μm and (B) 100 nm.

Core-Shell Structure of the Nanoparticles

Figure 6 displays ζ-potential curves of ovalbumin, lysozyme, and their mixture with MR 0.4, and the particles produced using standard process. The native lysozyme molecules are too small to be detected, and heat-denatured lysozyme solution, in which some aggregates existed, was used in ζ-potential measurement. Therefore, the ζ-potential data of lysozyme can

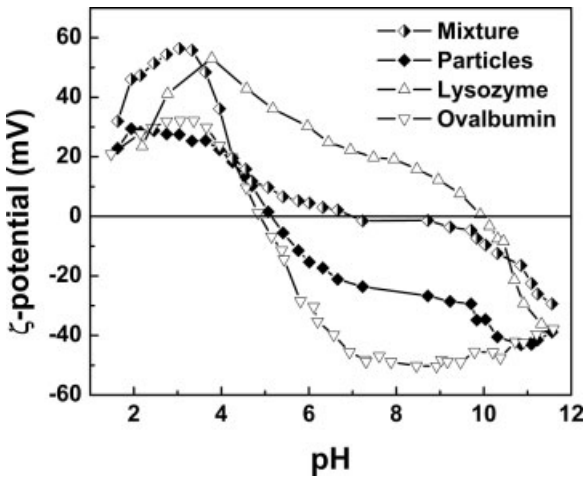

FIGURE 6 ζ-Potentials of ovalbumin, lysozyme, their mixture with MR 0.4, and the particles with MR 0.4 produced using the standard method.

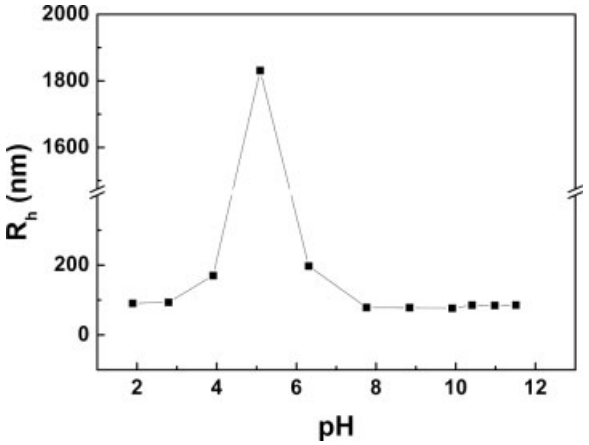

FIGURE 7 The pH dependence of the hydrodynamic radius of the particles. The particle sample was prepared using the standard method.

only be used qualitatively. The ζ-potential of the mixture is zero at pH 7.0, which is close to the average pH value of the zero ζ-potentials of the individual ovalbumin and lysozyme. However, the ζ-potential curve of the particles with MR 0.4 is different from the corresponding mixture and it is closer to the curve of ovalbumin: the particles carry net positive charges when pH is lower than 5.2 and carry net negative charges when pH is higher than 5.2. These results suggest that ovalbumin molecules are enriched on the particle surface and lysozyme molecules are shielded by ovalbumin molecules; therefore, lysozyme molecules cannot influence the ζ-potential of the particles significantly. Compared with the ζ-potential curves of the mixture and the corresponding particle solution, we can conclude that a molecular rearrangement in which ovalbumin molecules transfer to the particle surface took place when the pH of the mixture was changed from 5.3 to 10.3 and subsequently the mixture heated.

The absolute value of the ζ-potential of the particles in the pH range of 3–7 is not large enough to stabilize the particles in the solution, so secondary aggregation and precipitation occur in this pH range (Figure 7). Interestingly, the precipitates can be redispersed when the pH of the solution is out of this range, i.e., the particles display a pH-dependent reversible aggregation–dispersion transition. On the other hand, the particles do not dissociate over the pH range we studied, and the particles do not change their size when the solution pH is changed from 7.5 to 11.6, where the electrostatic attraction between ovalbumin and lysozyme is changed to electrostatic repulsion. As mentioned above, there are intermolecular hydrophobic interactions, disulfide bonds, and hydrogen bonds formed on heating the protein solution,[18,25] that is, every globular protein molecule is linked by the multiple intermolecular interactions in the particles. So it is understandable that the particles can keep their structure even if there is electrostatic repulsion inside.

High flow ultrafiltration membrane (molecular weight cutoff: 1×10^5) was used to separate the free protein molecules, if there is any, from the particles. The filtrate, the original particle solution, the individual ovalbumin and lysozyme solution were analyzed with SDS-PAGE after the samples were treated by the sample-loading buffer containing SDS and β-mercaptoethanol to break intermolecular hydrophobic interaction and disulfide bonds.[36] Two batches of the particle samples and their corresponding filtrates were prepared, and SDS-PAGE analysis results are shown in Figure 8. The sample concentrations were 2.0 mg/mL for ovalbumin, lysozyme, and particle-dispersed solution, respectively. The sample volume was 20.0 μL for each sample lane. Figure 8 shows that no protein can be detected in the filtrate lane,

FIGURE 8 SDS-PAGE analysis of individual ovalbumin and lysozyme solution, the particle solutions, and their corresponding filtrates. The particle samples prepared using the standard method were filtrated through ultrafiltration membrane (molecular weight cutoff: 1×10^5). The samples are ovalbumin (lane 1), lysozyme (lane 2), particle solutions (lane 3, 6), and the corresponding filtrates of the particles (lane 4, 7). Lane 5 is molecular marker (14.4, 18.4, 25.0, 35.0, 45.0, 66.2, 116.0 kDa).

which means that all the protein molecules have taken part in the assembly. For the particle solution lane, only the ovalbumin band appears; the remains appear in the sample hole and they are too large to enter the stack gel. The amount of ovalbumin band appearing in the particle lane is about 70% analyzed using the standard gray scale analysis method.

In our study, we found that the electrophoresis results were similar for the particle samples treated with SDS and β-mercaptoethanol loading buffer for different times, that is, about 70% ovalbumin came off from the particles. To further clarify that only ovalbumin can come off when the sample reaches equilibrium, another method was used: the particle sample reacted with 0.5% SDS and 10 m*M* reducing agent DL-dithiothreitol (DTT) for different times to break down the hydrophobic interaction and disulfide bonds,[37] then DLS measurement was performed. For the sample reacted with SDS and DTT for less than 1 h, the R_h increases from 68 to 115 nm and the intensity decreases from 163 to 92 Kcps compared with the original particle sample. After treating the sample with SDS and DTT for 48 h, the intensity further decreases to 67 Kcps and R_h further increases to 128 nm. The larger R_h and the weaker intensity imply that the particles aggregate and the particle number decreases after treating with SDS and DTT.

As we know, pH 10.3 is close to the pI of lysozyme but far from the pI of ovalbumin; therefore, the gel structure of ovalbumin is much looser and weaker than that of lysozyme, according to the globular protein gelation theory.[26] Obviously, ovalbumin gel is easier while lysozyme gel is hard to break down by SDS and DTT/β-mercaptoethanol. Only 70% ovalbumin can come off from the particles, suggesting that 70% ovalbumin molecules are in the shell of the particles and can react with SDS and DTT, and the other ovalbumin molecules may be trapped in the lysozyme networks. After ovalbumin molecules in the shell of the particles came off, the particle core did not carry enough net charges at pH 10.3 and secondary aggregation happened, resulting in the increase of R_h and the decrease of the intensity. This result indicates that ovalbumin molecules preferentially locate on the particle surface while lysozyme molecules preferentially locate in the core of the particles. This conclusion is consistent with the fact that the ζ-potential curve of the particles is closer to that of ovalbumin (Figure 6).

DISCUSSION

Figure 2 shows that aggregation peak begins to appear after 120 min of stirring. More and larger aggregates appear when further increasing the stirring time. After 330 min of stirring, macroscopical coagulation appears. The SDS-PAGE result shows that about 10% of ovalbumin molecules are detected in the filtrate lane of the sample with 120 min of stirring (data not shown), suggesting that about 10% free ovalbumin molecules exist in the particle dispersion. Increasing the stirring time further, free ovalbumin molecules increase in the particle solution. Combining this with DLS and SDS-PAGE results, we can conclude that the homogeneous ovalbumin–lysozyme complexes formed during the process of changing mixture pH from acidic to neutral play an important role in the particle formation. The complexes undergo a molecular rearrangement at pH 10.3: there is no significant electrostatic attraction between negatively charged ovalbumin and about zero-charged lysozyme, so ovalbumin molecules tend to keep away from each other while lysozyme molecules tend to associate. If ovalbumin–lysozyme complexes formed at neutral pH are left at pH 10.3 for more than 330 min, the decrease of ovalbumin molecules in the complexes results in coagulation after heat treatment. This result is similar to the case of mixing the two proteins directly at pH 10.3 and then heating the mixture. In our particle preparation, the ovalbumin–lysozyme complex solution was heated at pH 10.3 after 60 min stirring, where lysozyme gelated to form a charge-neutral core and the peripheral ovalbumin molecules which carry large amount of negative charges prevented lysozyme molecules from coagulation.

The behavior of the particles in physiological pH 7.4 PBS solution (10 m*M* phosphate buffer with 160 m*M* ionic strength) was studied. The DLS result shows that the particle size distribution with an average R_h of 92 nm is similar to that in pH 7.4 salt-free water, implying that the particles are stable and do not aggregate in physiological condition. In addition, we conjugated dextran to the surface of the particles with Maillard reaction[38] to improve the dispersibility of the particles in the pH range of 3–7. The results show that the particles conjugated with dextran are dispersible in the pH range we studied and their size is about 80 nm. The details of dextran-modified particles will be published elsewhere.

The particles have a lysozyme-rich core and a ovalbumin-rich shell structure; therefore, the charges of the core and shell depend on the medium pH: both core and shell carry positive charges at pH less than 5 and negative charges at pH higher than 10; at pH around 5 the net charge of the shell is about zero; at a pH range from 5–10 the core carries positive charges and the shell carries negative charges (Scheme 2). The hydrophobicity/hydrophilicity of the particles was

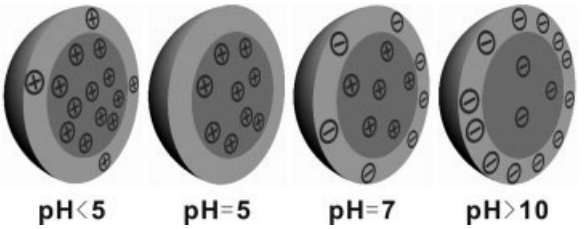

SCHEME 2 Illustration of the charge changes of the nanogels at different pHs.

investigated by examining the intensity ratio of the first to third band (I_1/I_3) in pyrene fluorescence emission spectrum.[39,40] The samples were prepared by adding pyrene to the particle dispersion to $10^{-7}M$ and the samples were left at 4°C for 48 h to reach equilibrium. The I_1/I_3 value is about 1.36, indicating a relatively hydrophobic environment of pyrene. Benzoic acid, which may interact with the particles through hydrophobic and electrostatic interactions, was used as a model drug. The loading was performed at pH 5 by adding 15 mg lyophilized particle powder into 10 mL of 0.1 mg/mL benzoic acid solution and then leaving the sample at 4°C for a few days. Ultraviolet-visible (UV-vis) absorption spectra show that benzoic acid can be loaded in the particles, suggesting that the particles are a candidate of drug carriers.

The method used in this study is convenient and effective. We have found that the mechanism can be applied to other oppositely charged protein pairs to prepare nanogels, such as bovine serum albumin–lysozyme, casein–lysozyme, α_S-casein–ovotransferrin, and ovalbumin–ovotransferrin. The detailed preparation condition for each pair is somewhat different from that for ovalbumin–lysozyme pair because the charges and the denaturation temperature of the proteins are different from each other. For ovalbumin–lysozyme nanogels, both ovalbumin and lysozyme are isolated from hen egg white and no chemicals are used except alkali in the preparation process so the nanogels are edible and nutritional. Furthermore, the nanogel solutions are very stable for long-time storage and the nanogels can be stored as lyophilized powder, so it is very convenient for application.

The financial support of the National Natural Science Foundation of China (NSFC Project 20474009 and 50333010) is gratefully acknowledged.

Supplemental Information. The calculation of *z*-averaged real hydrodynamic radius and *z*-averaged root mean square radius of gyration and *z*-averaged apparent hydrodynamic radius are presented in Supplemental Information.

REFERENCES

1. Goodsell, D. S. Bionanotechnology: Lessons from Nature; John Wiley & Sons: New York, 2004.
2. Kiser, P. F.; Wilson, G.; Needham, D. Nature 1998, 394, 459–462.
3. Rosler, A.; Vandermeulen, G. W. M.; Klok, H. A. Adv Drug Deliver Rev 2001, 53, 95–108.
4. Elemans, J. A. A. W.; Rowan, A. E.; Nolte, R. J. M. J Mater Chem 2003, 13, 2661–2670.
5. Savic, R.; Luo, L. B.; Eisenberg, A.; Maysinger, D. Science 2003, 300, 615–618.
6. Yang, L. H.; Liang, H. J.; Angelini, T. E.; Butler, J.; Coridan, R.; Tang, J. X.; Wong, G. C. L. Nat Mater 2004, 3, 615–619.
7. Bellomo, E. G.; Wyrsta, M. D.; Pakstis, L.; Pochan, D. J.; Deming, T. J. Nat Mater 2004, 3, 244–248.
8. Harada, A.; Kataoka, K. J Controlled Release 2001, 72, 85–91.
9. Vauthey, S.; Santoso, S.; Gong, H. Y.; Watson, N.; Zhang, S. G. P Natl Acad Sci USA 2002, 99, 5355–5360.
10. Koltover, I. Nat Mater 2004, 3, 584–586.
11. Clark, J.; Singer, E. M.; Korns, D. R.; Smith, S. S. Biotechniques 2004, 36, 992–1001.
12. Reedy, C. J.; Gibney, B. R. Chem Rev 2004, 104, 617–649.
13. Cao, R.; Gu, Z. Y.; Hsu, L.; Patterson, G. D.; Armitage, B. A. J Am Chem Soc 2003, 125, 10250–10256.
14. Cao, R.; Gu, Z. Y.; Patterson, G. D.; Armitage, B. A. J Am Chem Soc 2004, 126, 726–727.
15. Veerman, C.; de Schiffart, G.; Sagis, L. M. C.; van der Linden, E. Int J Biol Macromol 2003, 33, 121–127.
16. Yonezawa, Y.; Tanaka, S.; Kubota, T.; Wakabayashi, K.; Yutani, K.; Fujiwara, S. J Mol Biol 2002, 323, 237–251.
17. Jimenez, J. L.; Nettleton, E. J.; Bouchard, M.; Robinson, C. V.; Dobson, C. M.; Saibil, H. R. P Natl Acad Sci USA 2002, 99, 9196–9201.
18. Mine, Y. Trends Food Sci Tech 1995, 6, 225–232.
19. Damodaran, S. In Food Proteins and Their Applications; Damodaran, S., Paraf, A., Eds.; Marcel Dekker: New York, 1997; pp 1–24.
20. Arntfield, S. D.; Bernatsky, A. J Agric Food Chem 1993, 41, 2291–2295.
21. Oakenfull, D.; Pearce, J.; Burley, R. W. In Food Proteins and Their Applications; Damodaran, S., Paraf, A., Eds.; Marcel Dekker: New York, 1997; pp 111–142.
22. Bronich, T. K.; Keifer, P. A.; Shlyakhtenko, L. S.; Kabanov, A. V. J Am Chem Soc 2005, 127, 8236–8237.
23. Eichenbaum, G. M.; Kiser, P. F.; Dobrynin, A. V.; Simon, S. A.; Needham, D. Macromolecules 1999, 32, 4867–4878.
24. Ibrahim, H. R.; Higashiguchi, S.; Juneja, L. R.; Kim, M.; Yamamoto, T. J Agric Food Chem 1996, 44, 1416–1423.
25. Matsudomi, N.; Yamamura, Y.; Kobayashi, K. Agric Biol Chem 1986, 50, 1389–1395.
26. Doi, E.; Kitabatake, N. In Food Proteins and Their Application; Damodaran, S., Paraf, A., Eds.; Marcel Dekker: New York, 1997; pp 325–340.

27. Tani, F.; Murata, M.; Higasa, T.; Goto, M.; Kitabatake, N.; Doi, E. J Agric Food Chem 1995, 43, 2325–2331.
28. Wu, C.; Zhou, S. Q. Phy Rev Lett 1996, 77, 3053–3055.
29. Deshiikan, S. R.; Papadopoulos, K. D. Colloid Polym Sci 1998, 276, 117–124.
30. Sarmiento, F.; Ruso, J. M.; Prieto, G.; Mosquera, V. Langmuir 1998, 14, 5725–5729.
31. Gonzalez-Perez, A.; Ruso, J. M.; Prieto, G.; Sarmiento, F. Colloid Polym Sci 2004, 282, 351–356.
32. Liu, G. M.; Zhang, G. Z. J Phy Chem B 2005, 109, 743–747.
33. Matsudomi, N.; Oka, H.; Sonoda, M. Food Res Int 2002, 35, 821–827.
34. Zhang, G. Z.; Winnik, F. M.; Wu, C. Phy Rev Lett 2003, 90, 035506-035501-035506-035504.
35. Yao, X. M.; Chen, D. Y.; Jiang, M. J Phy Chem B 2004, 108, 5225–5229.
36. Laemmli, U. K. Nature 1970, 227, 680–685.
37. Careche, M.; Alvarez, C.; Tejada, M. J Agric Food Chem 1995, 43, 1002–1010.
38. Fayle, S. E.; Gerrard, J. A. The Maillard Reaction; The Royal Society of Chemistry: Cambridge, 2002; pp 1–7.
39. Kalyanasundaram, K.; Thomas, J. K. J Am Chem Soc 1977, 99, 2039–2044.
40. Li, M.; Jiang, M.; Wu, C. J Polym Sci Part B: Polym Phys 1997, 35, 1593–1599.

Reviewing Editor: David Tirrell